Mathematical Epidemiology through Transport Phenomena Viewpoint: Generalized Coordinates to Categorize People and Preliminary Numerical Results towards COVID-19

Carlos A. Valentim[a], Naila A. Oliveira[b], Sergio A. David[c], José A. Rabi[c*]

[a] *Graduate Program in Materials Science and Engineering, University of São Paulo (USP) – Pirassununga campus, Brazil.*
[b] *Nursing Course, University Center "Max Planck" (UniMax), Indaiatuba, Brazil.*
[c] *Department of Biosystems Engineering, University of São Paulo (USP) – Pirassununga campus, Pirassununga, Brazil.*

[*]**Corresponding Author**: jrabi@usp.br

Received: 13 April 2021; Revised: 10 May; Accepted: 05 June; Published: 22 June 2021

Abstract: With historical roots linked to life sciences, species diffusion has inspired dynamic models for infectious disease spreading. However, drawbacks have been raised towards the inclusion of people's displacement effects, whose ordered motion might refer to species convection within transport phenomena perspective. By transcending usual geometric role of spatial coordinates, the present work proposes a surrogate mathematical description via dimensionless generalized coordinates as intended to categorize people, whether or not infected, in terms of age and comorbidities. Accordingly, while diffusive infection refers to random motion of categorized people, convective infection can be additionally invoked and assigned to "streamwise" (i.e. ontology-driven) people's motion. With infected-people fraction as dimensionless dependent variable, the governing partial differential equation equally considers source and sink terms referring respectively to contamination-reinfection and recovery-death rates. Such epidemic transport model is preliminary applied to SARS-CoV-2 spreading (i.e. COVID-19 dynamics) among categorized people and trial numerical simulations are performed in view of extant infection data from Florida (USA), here taken as case study. Prospective extensions for the proposed epidemic transport model are addressed (e.g. diffusive infection in inhomogeneous media and human's displacement rheology).

Keywords: Population modeling; Infectious disease dynamics; Epidemic modeling; General transport equation; Numerical simulation.

1. Introduction

Caused by new severe acute respiratory syndrome coronavirus 2 (SARS-CoV-2), COVID-19 was first identified in December 2019 as patients were diagnosed with unknown-origin pneumonia in Wuhan, China (Wiersinga et al., 2020). By generating a range of diseases in humans (e.g. respiratory, gastrointestinal or neurological diseases), coronaviruses are large enveloped single-stranded RNA viruses found in either humans or other mammals (e.g. dogs, cats, chickens, cattle, pigs, and birds). Coronaviruses typically tackled in clinical practice

include 229E, OC43, NL63 and HKU1, which generally bring about usual cold symptoms in immunocompetent individuals.

SARS-CoV-2 is the third coronavirus globally spread in the past two decades (Zhu et al., 2020). With its pandemic recognized on March 11 2020 (WHO, 2020a), COVID-19 has precipitously and significantly increased the number of pneumonia hospitalizations, along with various disease. COVID-19 infection can be asymptomatic or evidenced by wide spectrum of symptoms ranging from upper respiratory tract infection to life-threatening sepsis.

Bearing in mind likely restricted access to health services, social distancing has been claimed as essential public health response to COVID-19 pandemic (Shen et al., 2020). As means to relieve pressure on health systems, social distancing aims at decreasing COVID-19 transmission, thus reducing the number of infected people to potentially spread SARS-CoV-2 (Binda et al., 2020).

Besides age, comorbidities with greater risk factors for negative evolution of COVID-19 (WHO, 2020b) include cardiovascular diseases (10.5% mortality rates), diabetes (7.3% mortality rates), chronic respiratory diseases (6.3% mortality rates), arterial hypertension (6.0% mortality rates) and cancer (5.6% mortality rates). Hospital mortality due to COVID-19 is usually about 15-20% but it might rise up to 40% among patients requiring admission to intensive care unit (ICU). In consideration of patients' age, hospital mortality ranges from less than 5% among patients under 40 years of age up to 35% for those aged 70 to 79 years while surpassing 60% for 80-89 years old patients (Richardson et al., 2020).

In view of that, relevant points in epidemiological models for pandemic diseases such as COVID-19 should include (but are definitely not restricted to) human ontology and/or comorbidities. A comprehensive mathematical framework should contemplate either cultural particularities or behavioral changes (Acuña-Zegarra et al., 2020) with respect to not only input model parameters or data but also in regard to output results or predictions.

Ultimately inspired by the long-standing work of (Kermack & McKendrick, 1927), compartmental models for epidemic spreading have recurrently relied on systems of ordinary differential equations (Bailey, 1975; Hethcote, 1989; Brauer & Castillo-Chávez, 2012; Blyuss & Kyrychko, 2021). In those models, people are allowed to 'flow' through different compartments (namely S = susceptible, E = exposed, I = infectious, R = recovered) so that labels indicate conceivable flow patterns (e.g. SIR, SIS, SEIR, SEIS, or SEIRS), which can be extended to include other compartments (e.g. P = prodromal cases, M = mildly symptomatic cases, H = cases requiring hospitalization, D = cases dying in hospital) (Overton et al. 2020). Despite people are actually moving around (i.e. changing their positions in space), dynamic epidemiologic models are usually of zero-order dependence on spatial coordinates.

While COVID-19 spread from contact surfaces (e.g. touching surfaces with viruses) is indeed a possible transmission mode, epidemiological studies have pointed to aerosols (i.e. small droplets suspended in the air) as major infection route. Hence, droplets expelled from speech, coughing and sneezing during face-to-face exposures comprise habitual transmission means. While aerosol spreading among humans remains feebly studied, estimates suggest that 48-62% COVID-19 transmission occurs through pre-symptomatic carriers (Wiersinga et al., 2020). Prolonged exposure to infected person (less than 2 m apart for at least 15 min) and shorter exposures to symptomatic individuals (e.g. coughing) are assigned to increased risk of transmission due to virus dispersion in aerosols.

Models inspired by reaction-diffusion processes have been proposed in mathematical epidemiology as well (Medlock, 2004; Ducrot and Magal, 2009; Belik et al., 2011). In those dynamic models, quantities depend not only on time but also on further independent variables and they become mathematically expressed in terms of partial differential equations (PDEs). In diffusion-like infectious disease models (Sabel et al., 2009), while cardinal directions have been assigned as independent variables, drawbacks have been pointed to proper incorporation of people's displacement effects (Medlock, 2004).

As exemplified in (David & Rabi, 2020), observable phenomena can be modeled by following alternative pathways. With respect to COVID-19 dynamics, time branching process may model outbreak early days (Levesque et al., 2021) whereas the reproductive number can indicate whether an emerging disease will become epidemic (Shaw and Kennedy, 2021). For infectious disease spreading, unusual approaches might extend reaction-diffusion epidemic models towards description via generalized coordinates (not restricted to their spatial role) as means to suitably include convective contribution to disease spreading.

As discussed in section 3.1, generalized coordinates are here envisaged to categorize people in terms of age, comorbidities, or social activity level. While age-structured transport equations have been used to model spatial dynamic of vole populations (Donadello et al., 2021), importance of categorizing individuals in heterogeneous populations for mathematical epidemiology purposes has been addressed in view of herd immunity to SARS-CoV-2 (Britton et al., 2020).

As far as population biology modeling is concerned, COVID-19 pandemic has received unprecedented attention (Rosenberg, 2021). Motivated by scientific 'what-if' impetus, the present work envisions a surrogate model pathway for mathematical epidemiology in terms of (dimensionless) generalized coordinates and transport phenomena. Accordingly, theoretical concepts are discussed next, followed by prospective connections and/or adjustments towards infectious disease spreading.

2. Transport equation of conserved quantities

Transport phenomena are triggered and upheld by concentration differences, where 'concentration' refers to some (say) 'abundance degree' of physical quantities under analysis (e.g. momentum, energy, chemical species, or electric charge). Those observable quantities allegedly follow universal conservation principles, which are conceived and mathematically expressed by considering assorted contributions to overall balance in a 'hosting' medium.

In transport phenomena, conservation balances may comprise diffusive contribution due to interactions between the transported quantity and the hosting medium as well as convective contribution from external actions on the hosting medium itself. Additionally, the transported quantity can be locally consumed and/or generated. As those phenomena concurrently occur, they are modeled altogether in the so-called transport equation – a classic PDE in which the transported quantity is a function of not only time but also spatial coordinates.

Often linked to scalar field transport in an incompressible flow, the transport equation describes how a physical quantity is transferred across its hosting medium. It can be seen as the generalization of continuity equation (Rodi, 2017) as this latter equation is limited to mass conservation while the convection-diffusion equation describes continuity and conservation of any scalar field in space (May, 2017).

The continuity principle stated that the variation rate of a scalar quantity in a differential control volume must account for flow as well as diffusion of such scalar, both into and out of this volume, along with generation and/or consumption rates therein. From the mathematical viewpoint (Peube, 2009), this balance is expressed by the following equation:

$$\frac{\partial \varphi}{\partial t} + \nabla \cdot \mathbf{j} = S_{\varphi} \tag{1}$$

where φ is the scalar field under analysis, **j** is φ-flux vector through volume boundaries (i.e., control surface), and S_{φ} comprises φ source/sink in the control volume. Mathematically, $\partial\varphi/\partial t$ gives the local variation rate of scalar quantity φ, $\nabla\cdot\mathbf{j}$ is the net φ-balance entering and exiting the control volume, and S_{φ} represents either φ generation or consumption inside the volume.

The transport equation, Eq. (1), can be further detailed by either developing or adapting its terms. Nonetheless, prior to discussing the prospective use of the transport equation in mathematical epidemiology, its underlying concepts are concisely discussed in what follows. For more details, the reader may refer to long-established textbooks on transport phenomena (Sissom and Pitts, 1972; Bennet and Myers, 1974; Bird et al., 2007).

2.1. Extensive and intensive quantities

Observable quantities can be categorized as either extensive or intensive. Values of the former depend on system extension such as area, volume, amount of matter, mass, and force. In opposition, values of intensive quantities might vary from point to point within the system such as pressure, stress, concentration, density, and temperature.

Extensive and intensive quantities can be interconnected. For example, suitably chosen for this work, let $\mathrm{d}N_i$ be the amount of some chemical species (here identified by subscript i) within a differential volume $\mathrm{d}V$ about a given point (i.e. spatial position) in a 3-D solution domain. From those two differential extensive quantities $\mathrm{d}N_i$ and $\mathrm{d}V$, species concentration C_i can be defined as:

$$C_i = \frac{\mathrm{d}N_i}{\mathrm{d}V} \tag{2}$$

which is an intensive quantity. Conversely, if species concentration C_i is point-to-point known in a given system volume V, its total amount N_i can be retrieved as:

$$N_i = \int \mathrm{d}N_i = \int C_i \, \mathrm{d}V \tag{3}$$

with the integration being performed over the whole system.

Two particularities are of interest at this point. Firstly, in 2-D domains those previous mathematical relations spatially reduce to:

$$C_i = \frac{\mathrm{d}N_i}{\mathrm{d}A} \quad \leftrightarrow \quad N_i = \int \mathrm{d}N_i = \int C_i \, \mathrm{d}A \tag{4}$$

where species concentration C_i is integrated on area-basis so as to provide the total amount N_i. Further simplification to 1-D (i.e. linear) domains is here omitted for brevity. Secondly, let $\mathrm{d}N$ be the total amount of all species within $\mathrm{d}V$ (or $\mathrm{d}A$) so that:

$$\mathrm{d}N = \sum_i \mathrm{d}N_i \quad \text{and} \quad N = \int \mathrm{d}N \tag{5}$$

where N is the total amount of all species within the system. Accordingly, it is sometimes convenient to mathematically describe species concentration in dimensionless form as:

$$\chi_i = \frac{\mathrm{d}N_i}{\mathrm{d}N} = \frac{\mathrm{d}N_i/\mathrm{d}V}{\mathrm{d}N/\mathrm{d}V} = \frac{C_i}{C} \tag{6}$$

where χ_i is referred to as species fraction (or amount fraction), which is an intensive quantity, whereas C is whole system concentration with all species included.

While some conservation laws (balance equations) are expressed in terms of variation rates of extensive quantities, detailed knowledge of intensive quantities is essential to retrieve their extensive counterparts. Moreover, it is precisely point-to-point description of intensive

quantities that may help spotting inefficiencies (i.e. undesired values) to be locally optimized. Comprehensive (i.e. point-to-point) mathematical description is achieved by putting forward and solving governing differential equations for intensive quantities (de Souza-Santos, 2010).

2.2. Continuum hypothesis

Equations (2)-(6) implicitly invoke the continuum hypothesis, which treats any medium as having no voids, i.e. a continuum solution domain. It prevails whenever a representative number of constituent elements populate any differential volume dV or area dA to the point where individual behaviors can be overlooked. In other words, the smallest dV or dA to validate the continuum hypothesis must have enough elements so that statistical average of their effects (e.g. on intensive quantities) no longer depends on their probabilistic state. Such smallest dV or dA is then referred to as a 'point' in the solution domain, being very small if compared to bulk system dimensions.

Under continuum hypothesis, any intensive quantity can be modeled as steadily varying in space and time (Barton, 1992; Ørstavik et al., 2000). In view of that, species fraction χ_i can be mathematically represented by a continuous function of position $\mathbf{r}$ and time t, which in 3-D Cartesian coordinates becomes:

$$\chi_i(\mathbf{r}, t) = \chi_i(x, y, z, t) \tag{7}$$

where $\mathbf{r} = x\mathbf{i} + y\mathbf{j} + z\mathbf{k}$, being $\mathbf{i}$, $\mathbf{j}$ and $\mathbf{k}$ orthogonal unit vectors. In 2-D model frameworks, one coordinate (say z) is declined while in 1-D model only one coordinate (e.g. x) remains.

2.3. Lagrangian and Eulerian specifications

Mathematical modeling of transport phenomena and/or fluid flow might follow distinct descriptions (Leal, 2007; Slattery at al., 2007). If individual elements (e.g. suspension particles) can be easily and unceasingly identified in the flow field, Lagrangian method can be invoked to pursue those elements in space and time. Formal description of individual trajectories requires 'labeling' all elements while tracking down their motion together with mutual interactions (if any).

Other than chasing constituent elements, specific positions (e.g. control points) in the solution domain can be observed over time as system dynamically evolves. This is the very spirit of Eulerian method, which aims at describing systems in terms of intensive quantities properly defined as functions of position and time. The mathematical idea of 'field' naturally arises as means to describe system dynamic evolution in terms of intensive quantities.

In a 'theatrical' metaphoric comparison, Lagrangian method is mostly concerned with the 'cast' or specific 'actors' whereas Eulerian method pays attention to the 'stage' or specific

places therein. However, and almost paradoxically, governing differential (balance) equations for intensive quantities (stepping-stone concepts in Eulerian method) are obtained from the Lagrangian description of a differential constituent element as it moves d**r** during advancing time step dt.

Abovementioned mathematical artifice leads to the material derivative operator D/Dt, also known as total or substantial derivative. Accordingly, if $\chi_i = \chi_i$ (**r**, t) is species fraction at position **r** and time t, its material derivative is defined as:

$$\frac{\mathrm{D}\chi_i}{\mathrm{D}t} = \frac{\partial \chi_i}{\partial t} + \mathbf{v} \cdot \nabla \chi_i \tag{8}$$

where **v** is suitably identified as flow velocity and ∇ is del (or nabla) operator here applied to fraction scalar field χ_i as gradient, i.e., $\nabla \chi_i = \text{grad}\ \chi_i$. In Cartesian coordinates, those two vector entities become expressed as:

$$\mathbf{v} = v_x \mathbf{i} + v_y \mathbf{j} + v_z \mathbf{k} \quad \text{and} \quad \nabla = \frac{\partial}{\partial x}\mathbf{i} + \frac{\partial}{\partial y}\mathbf{j} + \frac{\partial}{\partial z}\mathbf{k} \tag{9}$$

This proper velocity identification holds for d$t \to 0$ as Lagrangian and Eulerian descriptions coincide or, by putting it another way, as particle trajectories (i.e. individual constituents' behavior) instantaneously coincide with flow streamlines (i.e. bulk medium's behavior).

2.4. Transport equation for intensive quantities

In a flowing hosting medium, governing differential equations for intensive quantities transported can be derived from conservation laws by following Eulerian method. In terms of material derivative, Eq. (8), the resulting transport equation can be adapted to fraction χ_i as:

$$\frac{\partial \chi_i}{\partial t} + \mathbf{v} \cdot \nabla \chi_i = \nabla \cdot \left(D_{i,m} \nabla \chi_i \right) + S_i \tag{10}$$

where $D_{i,\,m}$ is the diffusivity of species 'i' in hosting medium 'm' (where it diffuses) and S_i refers to either source or sink rates. Table 1 summarizes possible interpretations and features of mathematical terms in Eq. (10). By assuming uniform diffusivity $D_{i,\,m}$ while splitting S_i into species generation and consumption rates, i.e., $S_i = S_{i,\text{gen}} - S_{i,\text{cons}}$, Eq. (10) in 2-D Cartesian coordinates becomes:

$$\frac{\partial \chi_i}{\partial t} + v_x \frac{\partial \chi_i}{\partial x} + v_y \frac{\partial \chi_i}{\partial y} = D_{i,m} \left(\frac{\partial^2 \chi_i}{\partial x^2} + \frac{\partial^2 \chi_i}{\partial y^2} \right) + S_{i,\text{gen}} - S_{i,\text{cons}} \tag{11}$$

Table 1: Interpretation of terms in the transport equation as adapted to species fraction

$\partial \chi_i / \partial t$	*Transient term*: refers to local variation of species fraction with respect to time. In steady-state scenarios this term is null (i.e. species fraction remains constant over time but still may vary from point to point in the solution domain).
$\mathbf{v} \cdot \nabla \chi_i$	*Convective term*: refers to streamwise transport due to orderly motion of the bulk (hosting) medium; therefore, it models how species are dragged to/from elsewhere. It is of parabolic nature (i.e. 1st-order spatial derivative) while modulated by bulk medium velocity.
$\nabla \cdot (D_{i,m} \nabla \chi_i)$	*Diffusive term*: refers to species transport due to local gradients in the bulk medium. It is of elliptic nature (2nd-order spatial derivative). If species diffusivity $D_{i,m}$ is spatially uniform (i.e., homogeneous), this term becomes written via Laplacian operator, $D_{i,m} \nabla^2 \chi_i$.
S_i	*Source/sink term*: it can be a collection of (and be split into) terms whose underlying nature is unrelated from other terms in the transport equation. Typically, it may refer to (i.e., be split into) local generation $S_{i,\text{gen}}$ and/or consumption $S_{i,\text{cons}}$ rates.

3. Transport equation towards mathematical epidemiology

In order to apply Eq. (10) to mathematical epidemiology, variables and parameters in this governing EDP should be reinterpreted under disease spreading viewpoint. In particular, this work puts forward a paradigm shift in terms of the prospective use of generalized coordinates in place of exclusively using geometric coordinates. The resulting governing EDP may be a springboard towards an 'epidemic transport model', whose adaptation to COVID-19 is here envisaged (in section 4).

3.1. Independent variables: time and generalized coordinates

When modeling infectious disease spreading, time t should render no misperception as independent variable while Cartesian coordinates could supposedly refer to cardinal directions in 2-D domains, e.g. x for west-east direction and y for south-north direction in Eq. (11). In transport phenomena, this spatially biased association forthrightly follows as the dimensions of flow velocity $\mathbf{v}$ and species diffusivity $D_{i,m}$ are respectively [length] [time]$^{-1}$ and [length]^2 [time]$^{-1}$, in principle.

By transcending their systematic geometric role, let independent variables x and y be assigned to (say) generalized coordinates, which must be suitably normalized for

dimensional consistency purposes. By rendering dimensionless coordinates, this normalization is two-fold necessary, namely:

- Streamwise velocity **v** can be alternatively interpreted as contamination velocity, whose multidimensional components are defined in terms of time and dimensionless generalized coordinates, thus with the same dimensions, namely [time]$^{-1}$ (section 3.3);
- Diffusivity $D_{i,m}$ become dimensionally consistent for any 'multidimensional generalized' domain as its dimensions simplify to [time]$^{-1}$, regardless of the generalized coordinates system (section 3.4).

In a dynamic 1-D model, for instance, generalized coordinate x could be associated to inhabitants' age as measured in some dimensionless continuous scale, e.g. normalized by life expectancy. In 2-D modeling, generalized coordinate y could be additionally assigned to any comorbidity related to COVID-19 in a suitable scale, e.g. obesity as measured through body mass index (BMI) prime. Defined as the ratio of actual BMI to optimal BMI upper limit, BMI prime indicates to what extent a person deviates from maximum optimal BMI, being indeed a dimensionless number, i.e. it is conveniently independent from units.

3.2. Dependent variables: infected people and infected fraction

Bearing in mind Eqs. (2)-(6), the epidemic transport model identifies N_i as the number of infected people among N inhabitants in a particular country, state, region, county or town. In this descending geographic order, can the analyzed system become as small as a district or neighborhood? As the continuum hypothesis must be properly fulfilled, care must be always exercised and, from now on, it is assumed the continuum hypothesis actually holds.

In the epidemic transport model, N_i and χ_i arise as dependent variables interrelated via Eq. (6). The former is an extensive variable depending only on time, i.e. $N_i = N_i(t)$, while the latter is an intensive dimensionless variable to be modeled as a continuous function of time and dimensionless generalized coordinates in line with Eq. (7).

At this point, the so-called 'diluted mixture' rationale is invoked so as to model infected people likewise diluted species transport in reactive medium (i.e. including generation and/or consumption rates). Consequently, $N =$ constant is assumed, which means that the dynamic size of the population under analysis is not severely affected by the infectious disease. In view of Eqs. (5) and (7), the instantaneous number of infected people in a given solution domain can be assessed as:

$$N_i(t) = N \int \chi_i(\mathbf{r}, t)\, \mathrm{d}\mathbf{r} \tag{12}$$

where the integration is performed over dimensionless generalized coordinates **r**. It is worth remembering that infected-people fraction χ_i is the transported intensive quantity that

comes from the solution of Eq. (10). In what follows, mathematical terms in this governing EDP are reinterpreted towards epidemic transport modeling.

3.3. Convective transport: 'streamwise' motion among categorized people

From fluid flow viewpoint, $\mathbf{v} = \mathbf{v}(\mathbf{r}, t)$ is the velocity vector field of the hosting medium as mathematically described through Eulerian specification. Therefore, the medium must be (or behave as) a fluid; otherwise $\mathbf{v} = 0$ for solid media, i.e. solids do not flow. Inherent to flowing media, convective transport is a macro-scale phenomenon as opposed to diffusive counterpart, which is micro-scale in nature and may occur in any medium, whether fluid or solid, as discussed ahead in section 3.4.

In Eq. (10), convective contribution $\mathbf{v}\cdot\nabla\chi_i$ must be reinterpreted in epidemic transport context. While paradigm shift from classic transport reasoning is envisaged, fluid dynamics may still serve as insight. At this point, two issues are brought to mind, namely:

- Contribution $\mathbf{v}\cdot\nabla\chi_i$ should be defined using dimensionless generalized coordinates, and
- Velocity $\mathbf{v}$ should refer to streamwise macro-scale motion of bulk hosting medium, opposed to random micro-scale motion of its constituent particles (leading to diffusion).

As proposed in section 3.1, dimensionless generalized coordinates may refer to age, BMI prime or any COVID-19 comorbidity in a suitable dimensionless scale. In other words, dimensionless generalized coordinates can categorize people, whether or not infected. As Eq. (9) evokes, components of velocity vector $\mathbf{v}$ can be themselves functions of dimensionless generalized coordinates (e.g., categorized people) and time, e.g., $v_x = v_x(\mathbf{r}, t)$. In the epidemic transport model, convective contribution $\mathbf{v}\cdot\nabla\chi_i$ should therefore refer to infectious disease spreading due to streamwise (i.e. organized) movement of categorized people as directed by contamination velocity vector $\mathbf{v}$.

A mathematical problem arises: how can contamination velocity vector $\mathbf{v}$ be modeled? Similar to its successful motivating role in electromagnetism, let fluid dynamics be inspiration again and this is where conceptual horizons become widely open. Not only fluid dynamics is a vast scientific branch itself but synergy with social sciences is envisioned to support proper choice or adaptation of flow rheology. In other words, contamination velocity $\mathbf{v}$ should be modeled in view of either cultural background or habits of categorized people. For details and prospective insights on convective transport and fluid flow, the reader may refer to (Kaviany, 1995; Kays et al., 2005; White, 2006; Nield and Bejan, 2017).

3.4. Diffusive transport: random motion among categorized people

If convection is inherent to bulk motion of a flowing medium in macro-scale perception, diffusion refers to chaotic motion of its constituent particles at micro-scale level. Specifically, convective transport is streamwise directed while diffusive transport is utterly driven by

concentration gradients. As a result, diffusion takes place regardless of any externally forced motion of the hosting medium. By putting it another way, diffusive and convective transport mechanisms are independent from each other to the point that they are indeed modeled as distinct terms in Eq. (10).

Diffusion spreads out the transported quantity from where it is highly concentrated towards lower concentration regions, i.e. opposed to the concentration gradient vector. This phenomenological description of diffusive transport aligns with Fick's law, but diffusion can be equally established in terms of 'random walks' of spreading particles, also referred to as Brownian motion. It is here interesting to realize that historical roots of diffusion are linked to life sciences: Adolf Fick (1829-1901) was a German physician and physiologist while Robert Brown (1773-1858) was a Scottish botanist and paleobotanist.

Fick's law of diffusion introduces a fundamental transport parameter, namely species diffusivity or diffusion coefficient. Prescribed pairwise with double indexes, $D_{i,m}$ indicates how fast a given species 'i' diffuses through a hosting medium 'm'. If the latter is spatially homogeneous (i.e. uniform), species diffusivity is a scalar property; otherwise, it becomes extended towards a tensor whose rank (order) depends on the number of diffusion directions invoked in the transport model. As Table 2 shows (Hines and Maddox, 1985; Cussler, 2009), uppermost diffusivities are observed in gases with orders of magnitude higher than values in liquids; the latter, in turn, being orders of magnitude higher than diffusivities in solids.

Table 2: Typical orders of magnitude of species diffusivities $D_{i,m}$ in gases, liquids, and solids

Diffusivity $D_{i,m}$ (i = species, m = medium)	**Typical order of magnitude (SI units)**
i = gas , m = gas	$\sim 10^{-5}$ m^2/s
i = liquid , m = liquid	$\sim 10^{-9}$ m^2/s
i = gas , m = solid	$\sim 10^{-10}$ - 10^{-13} m^2/s
i = solid , m = solid	$\sim 10^{-19}$ - 10^{-34} m^2/s

In the epidemic transport model, diffusive contribution $\nabla\cdot(D_{i,m}\nabla\chi_i)$ should thus refer to infectious disease spreading due to random (i.e. disorganized) motion of categorized people as dictated by species diffusivity $D_{i,m}$ depending on hosting medium (modeled as a continuum of categorized people). Hence, infectious disease transport via diffusion results from casual interactions among categorized people. For details and possibly insights, the reader may refer to specialized textbooks (Skelland, 1974; Crank, 1975).

3.5. Source and sink terms: contamination/reinfection and recovery/death rates

Besides convective and diffusive contributions as previously discussed, the epidemic transport model should equally consider the influence of either source or sink terms. Within the framework of Eq. (11), generation term $S_{i,\mathrm{gen}}$ can be associated to contamination and/or reinfection rates whereas consumption term $S_{i,\mathrm{cons}}$ should refer to recovery and/or death rates. Those terms can be functions of not only time and/or dimensionless generalized coordinates but also of infected fraction χ_i itself.

3.6. Initial and boundary conditions: known or estimated values

Initial and boundary conditions are required to solve Eq. (10). Initial conditions refer to a priori known or estimated infected fraction distribution if $\chi_{i,0} = \chi_i(\mathbf{r},0)$ in the solution domain at some reference date, which is then identified as initial instant $t = 0$.

As far as boundary conditions are concerned, the imposition of linear mathematical relations at domain border $\delta\Omega$ is particularly helpful (Riley et al., 2006; Kreyszig, 2011). In the epidemic transport model, boundary conditions can be imposed (over the considered time interval) as follows:

- Dirichlet condition specifies known or estimated value of infected fraction, i.e. $\chi_{i,\delta\Omega} = \chi_i(\delta\Omega,t)$;
- Neumann condition specifies known or estimated value of normal derivative of infected fraction, i.e. $(\partial\chi_i/\partial\mathbf{n})_{\delta\Omega} = (\mathbf{n}\cdot\nabla\chi_i)_{\delta\Omega} = \mathrm{f}(\delta\Omega,t)$;
- Robin condition specifies a weighted average (i.e. linear combination) of known or estimated values of infected fraction and its normal derivative.

Somehow resembling the latest boundary condition, Cauchy condition separately specifies function as well as its normal derivative at solution domain border. Last but not least, in transport phenomena involving fluid flow, Danckwerts condition can be alternatively imposed (Danckwerts, 1953).

4. Results and discussion

4.1. Preliminary dynamic 2-D epidemic transport model: COVID-19 pandemic

As any model in mathematical epidemiology, the epidemic transport model put forward in the present work is intended to be applied to infectious disease spreading in general. Due to its disquieting pandemic aspect, a pilot application was attempted to COVID-19. Prospective COVID-19 spreading from an initial scenario related to total infections in Florida (USA) on July 20th 2020, which refers to first-wave infection peak (Bevand, 2020; Florida Department of Health, 2020), was taken as case study. COVID-19 infection evolution was numerically

simulated by relying on the envisaged dynamic 2-D epidemic transport model, i.e., COVID-19 spreading dynamics was virtualized by means of Eq. (10) as governing PDE adapted to case study assumptions.

4.2. Statistical data to fine-tune epidemic transport model parameters

While the proposed epidemic transport model conceptually relies on phenomenological governing equations, the latter invoke parameters whose values are prone to be statistically determined. As claimed in (Saguy, 2016), a modeling paradigm shift is expected in which experimental data will support deterministic equations more willingly than observation-based models whose application scope tends to be more limited when compared to physics-based counterparts (de Souza-Santos, 2010).

In mathematical epidemiology, such a mechanistic-statistical model combination turns out to be manifest (if not necessary) as ethnical, socio-cultural, economic and even political issues become influential. Human mobility and control measures (Kraemer et al., 2020) along with geographic heterogeneity and its resulting spatial dynamics (Medlock, 2004) are among ascendant aspects in epidemiological systems. As human ontology may affect free parameters invoked in Eq. (11), some (interdisciplinary) modeling challenges arise.

As cited in section 1, the model framework here proposed is a surrogate mathematical pathway adapting transport phenomena concepts and equations towards epidemiology. To the best of authors' knowledge, the present work innovatively employs dimensionless generalized coordinates to categorize people in the governing transport-like PDE, whose parameters may be inferred with (say) synergic help from either Health or Social Sciences.

Nevertheless, as far as COVID-19 pandemic is concerned, statistical data characterizing infected people are more common in terms of hospital mortality than with respect to disease spreading dynamics. In (Baqui et al., 2020), a thorough cross-sectional observational study assessed COVID-19 mortality in Brazil according to patients' geographic region, ethnicity, comorbidities, and symptoms. In (Docherty et al., 2021), a recent multicenter observational cohort study was carried out to characterize COVID-19 first-wave mortality in the UK. Yet, such dataset can be helpful to infer source and sink terms ($S_{i,\mathrm{gen}}$ and $S_{i,\mathrm{cons}}$) in Eq. (11).

In the proposed epidemic transport model, diffusivity $D_{i,m}$ accounts for disorganized (i.e., random) infection among categorized people. This is a surrogate interpretation for such transport parameter, whose value is a priori unknown. While infection-recovery (i.e. source-sink) balance can be assumed for simplicity purposes (as discussed next), infected people can still move around casually. Hence, a tentative $D_{i,m}$ value should measure how fast COVID-19 randomly spreads (i.e., diffuses) among people.

Bearing in mind COVID-19 pathogenicity (Hamid et al., 2020), $D_{i,m}$ can be preliminary estimated in view of SARS-CoV-2 incubation and recovery time, which statistically leads to two weeks on average per single person (WHO, 2020c). As diffusivity dimensions simplify to [time]$^{-1}$ in the proposed epidemic transport model, the primary case study in the present work then assumes (per thousand of inhabitants):

$$D_{i,m} = \frac{1}{14\ \text{days}} \times \frac{1}{1000} \quad \rightarrow \quad D_{i,m} \cong 7.14 \times 10^{-5}\ \text{day}^{-1} \tag{13}$$

In line with time units in Eq. (13), advancing time step was set as $\Delta t = 1$ day in simulations.

4.3. Independent and dependent variables

Besides time t, independent variables comprised dimensionless generalized coordinates x and y respectively associated to inhabitants' age as normalized to life expectancy in Florida and BMI prime. Referring to dependent variables in Eq. (12), infected fraction $\chi_i = \chi_i(x, y, t)$ is expressed as total COVID-19 infections per thousand inhabitants for numerical convenience.

A typical solution domain might contain inhabitants whose ages range from 0 to 100 years and whose BMI range from 10 to 50 kg/m^2. By rounding off life expectancy in Florida as ~80 years (Florida Department of Health, 2019) while taking maximum optimal BMI as 25 kg/m^2 (Gadzik, 2006), solution domain resulted as $0 < x < 1.25$ and $0.4 < y < 2.0$ in terms of dimensionless generalized coordinates. Border values ($x = 0$, $x = 1.25$, $y = 0.4$, $y = 2.0$) were excluded from the solution domain as boundary conditions are imposed there. For numerical and data-related purposes, each dimensionless generalized coordinate x and y was discretized into 22 grid points (= 21 subdivisions).

4.4. COVID-19: initial infection scenario

In regard to initial condition $\chi_{i,0} = \chi_i(x, y, 0)$, input data referred to actual distribution of infected people per thousand inhabitants for different ages, in Florida on July 20th, 2020 (here taken as $t = 0$), as shown in Figure 1 in dimensionless values. As far as infection distribution in terms of BMI prime is concerned, literature lacks extant data to the best of our knowledge (this issue is resumed in section 4.6). In order to overcome this drawback, a function $f = f(x, y)$ correlating and distributing age-stratified real data x with respect to dimensionless BMI prime y was envisaged as follows:

$$f(x, y) = sin(y - 0.4)A(x)\frac{\Delta y}{N-1} \tag{14}$$

where $A(x)$ is the number of infected people per age subdivision, as given in Figure 1, while $\Delta y/(N-1)$ scales such value to each y-domain subdivision.

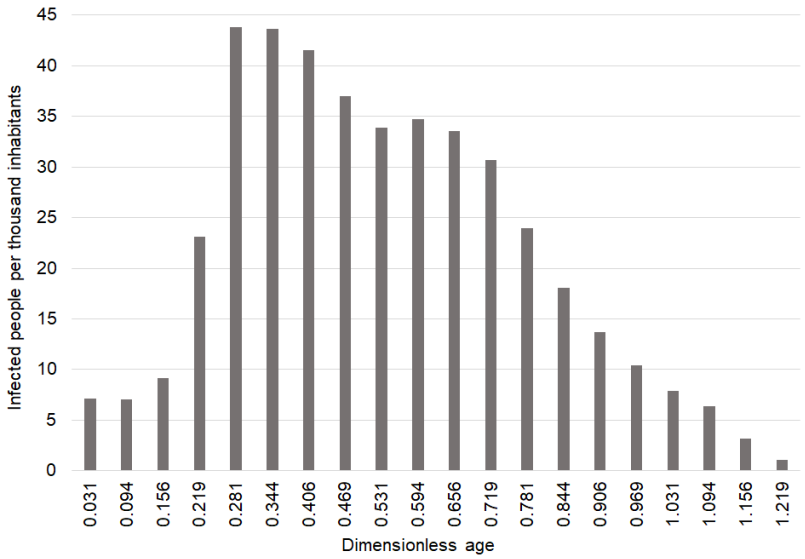

Figure 1: Data related to COVID-19 infected people per 1000 inhabitants in Florida on July 20th 2020, as distributed in terms of dimensionless age (= actual age / life expectancy)

Although the proposed distribution regarding BMI prime (y coordinate) is an estimate, for checking purposes real data of total infection according to age (x coordinate) can be can retrieved by integrating function f(x,y) with respect to y for each x subdivision. Figure 2 depicts the initial condition as adapted to the dimensionless domain discretization.

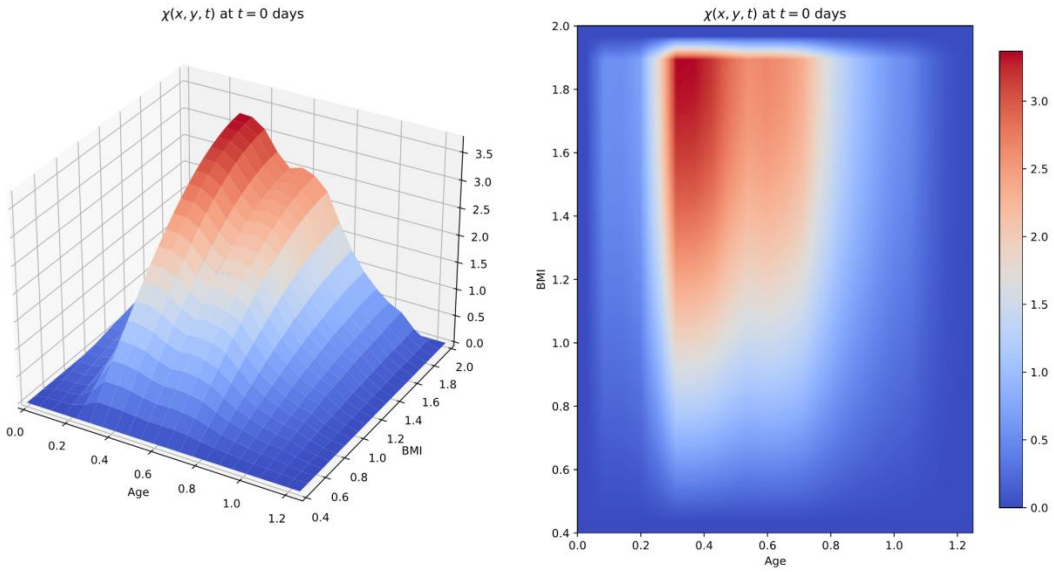

Figure 2: Initial condition $\chi_{i0} = \chi_i(x, y, 0)$: estimated fraction of COVID-19 infected people per 1000 inhabitants in Florida on July 20th, 2020, for dimensionless age and BMI prime

4.5. COVID-19 spreading under lockdown: 'perfect isolation' and 'healthy perimeter'

As pilot dynamic 2-D case study, COVID-19 spreading was numerically simulated for rigorous lockdown. This might be considered as a reference scenario where both traveling and ordered displacements are the lowest possible so that streamwise infection among categorized people is disregarded. Mathematically, convective contribution is negligible in comparison to diffusive counterpart, i.e., $\mathbf{v}\cdot\nabla\chi_i << \nabla\cdot(D_{i,m}\nabla\chi_i)$. Furthermore, let contamination-reinfection rates be roughly counterbalanced by recovery-death rates (in the delineated region). In such model simplification, source and sink terms are in dynamic equilibrium, i.e., $S_{i,\text{gen}} \approx S_{i,\text{cons}}$, which dismisses additional input data.

By further assuming homogeneous (uniform) hosting medium, Eq. (11) simplifies to:

$$\frac{\partial\chi_i}{\partial t} = D_{i,m}\left(\frac{\partial^2\chi_i}{\partial x^2} + \frac{\partial^2\chi_i}{\partial y^2}\right) \tag{15}$$

so that diffusivity $D_{i,m}$ is the only model parameter. While Eq. (15) is mathematically similar (if not equivalent) to governing PDEs in reaction-diffusion epidemiological models (Medlock, 2004; Ducrot and Magal, 2009; Sabel et al., 2009; Belik et al., 2011), it is worth stressing that independent variables x and y now refer to dimensionless generalized coordinates rather than being limited to spatial coordinates.

With respect to boundary conditions, the same type was numerically implemented at all borders for simplicity. Specifically in this work, either Dirichlet or Neumann boundary condition was tentatively imposed at a time so that two sets of numerical simulations were performed, one for each type. As those two boundary conditions have been long invoked in transport phenomena (Morse and Feshbach, 1953), they are prone to render familiar links in view of the introductory epidemiological interpretation herein proposed.

In the first set of numerical simulations, null Neumann condition was imposed at all boundaries (for $t > 0$), namely:

$$\left.\frac{\partial\chi_i}{\partial x}\right|_{y=0.4} = \left.\frac{\partial\chi_i}{\partial x}\right|_{y=2.0} = 0 \quad \text{and} \quad \left.\frac{\partial\chi_i}{\partial y}\right|_{x=0} = \left.\frac{\partial\chi_i}{\partial y}\right|_{x=1.25} = 0 \tag{16}$$

As this is mathematically equivalent to impermeable or adiabatic walls as far as mass and heat transfer are respectively concerned, Eq. (16) could be regarded as 'perfect isolation', meaning that disease spreading is confined within domain borders but infection itself is not effectively mitigated therein. This has been indeed invoked in epidemiological studies (Aniţa and Aniţa, 2005; Dai and Liu, 2020) to model effective physical barrier as 'cordon sanitaire' such as the one attempted in Wuhan, China (WHO, 2020c).

In the context of the generalized coordinates herein envisaged, null Neumann condition would impose that infectious disease would not spread across certain age or BMI groups.

Categorized people at solution domain edges would be effectively isolated (e.g. through social distancing) whereas economically active people at domain center would continue transmitting and being infected among themselves. This approach could model epidemiological scenarios where infectious disease remains restricted within specific groups as in (Monod et al., 2021).

The sequence in Figure 3 shows the potential dynamic evolution of infected fraction χ_i if isolation condition is assumed. It is noted that χ_i slowly equalizes among people of different ages and BMI prime, taking more than 6000 days (~ 16.5 years) to asymptotically reach uniform (endemic) infection, i.e. all categorized people become homogeneously infected. Though exaggerated, this outcome should not be surprising in view of a hypothetical scenario where no mitigation health measures are effectively undertaken other than simply balancing infection-recovery rates.

In the second set of simulations, null Dirichlet condition was imposed at all boundaries (for $t > 0$), meaning that infection beyond domain borders is negligible, namely:

$$\chi_i(x, y = 0.4, t) = \chi_i(x, y = 2.0, t) = 0 \quad \text{and} \quad \chi_i(x = 0, y, t) = \chi_i(x = 1.25, y, t) = 0 \quad (17)$$

Though less common, Dirichlet boundary condition can also be invoked in epidemiological models, in cases when the model framework establishes disease-free zones (Chekroun and Kuniya, 2020).

While it should be realized that borders are actually open, Eq. (17) could be possibly interpreted as creating (say) a 'healthy perimeter' (i.e. zero-infection perimeter) around categorized people. This approach could model a scenario in which specific age and BMI groups (i.e. priority groups) are under vaccination (thus effectively in zero-infection perimeter) whereas several economically active people are not yet, which is an actual scenario currently prevailing in many countries.

The sequence in Figure 4 shows the prospective dynamic evolution of infected fraction χ_i if 'healthy perimeter' condition is assumed. It is noted that while χ_i slowly equalizes among different people, it is also mitigated towards infection-free situation, which can indeed be evoked after 2000 days (~ 5.5 years). Again, this numerical simulation refers to a hypothetical scenario that assumes a dynamic balance between contamination-reinfection and recovery-death rates.

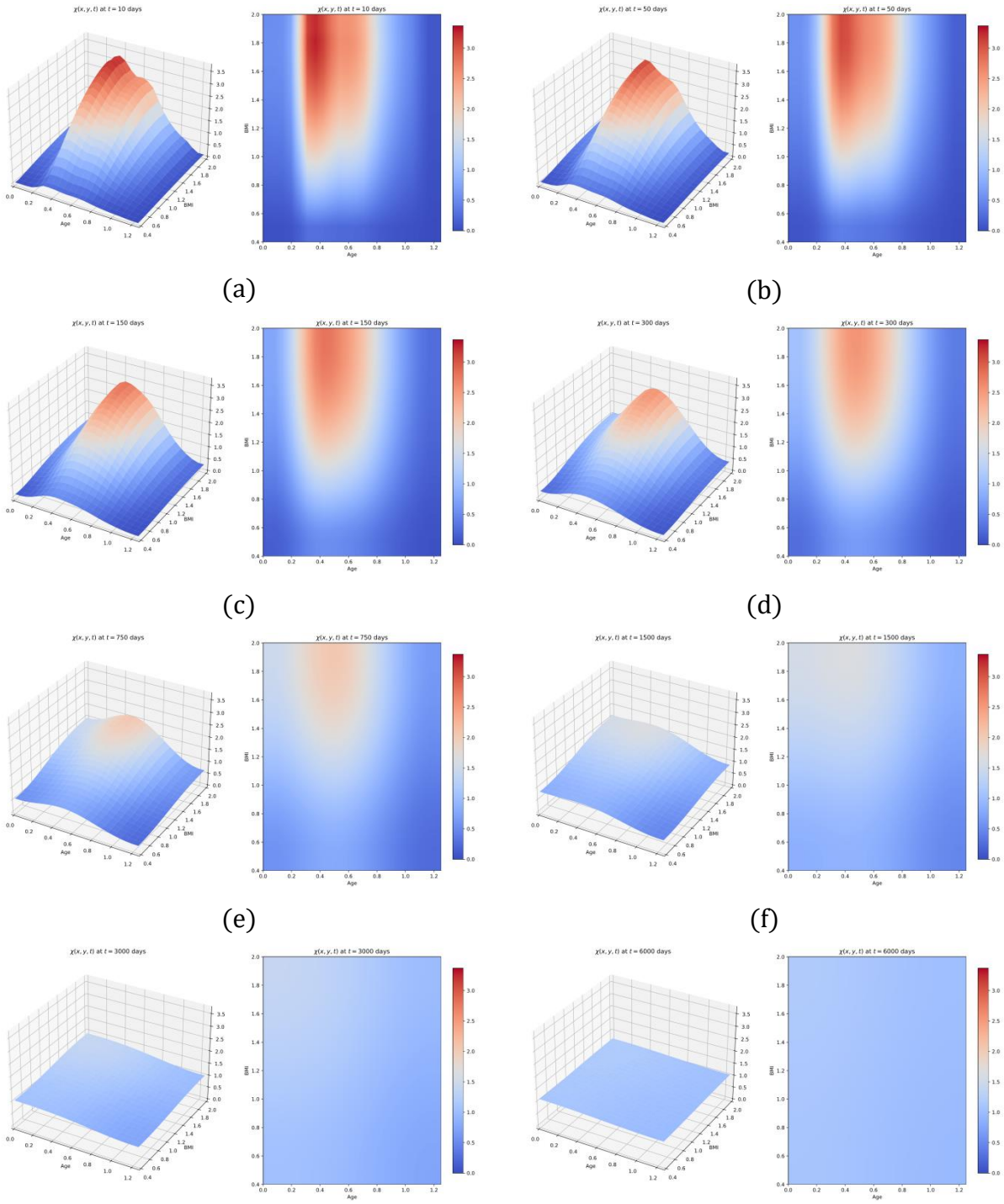

Figure 3: Prospective dynamic evolution of COVID-19 infected fraction $\chi_i = \chi_i(x,y,t)$ as numerically simulated by imposing null Neumann condition at all domain boundaries ('perfect isolation') after: (a) 10 days, (b) 50 days, (c) 150 days, (d) 300 days, (e) 750 days, (f) 1500 days, (g) 3000 days, (h) 6000 days

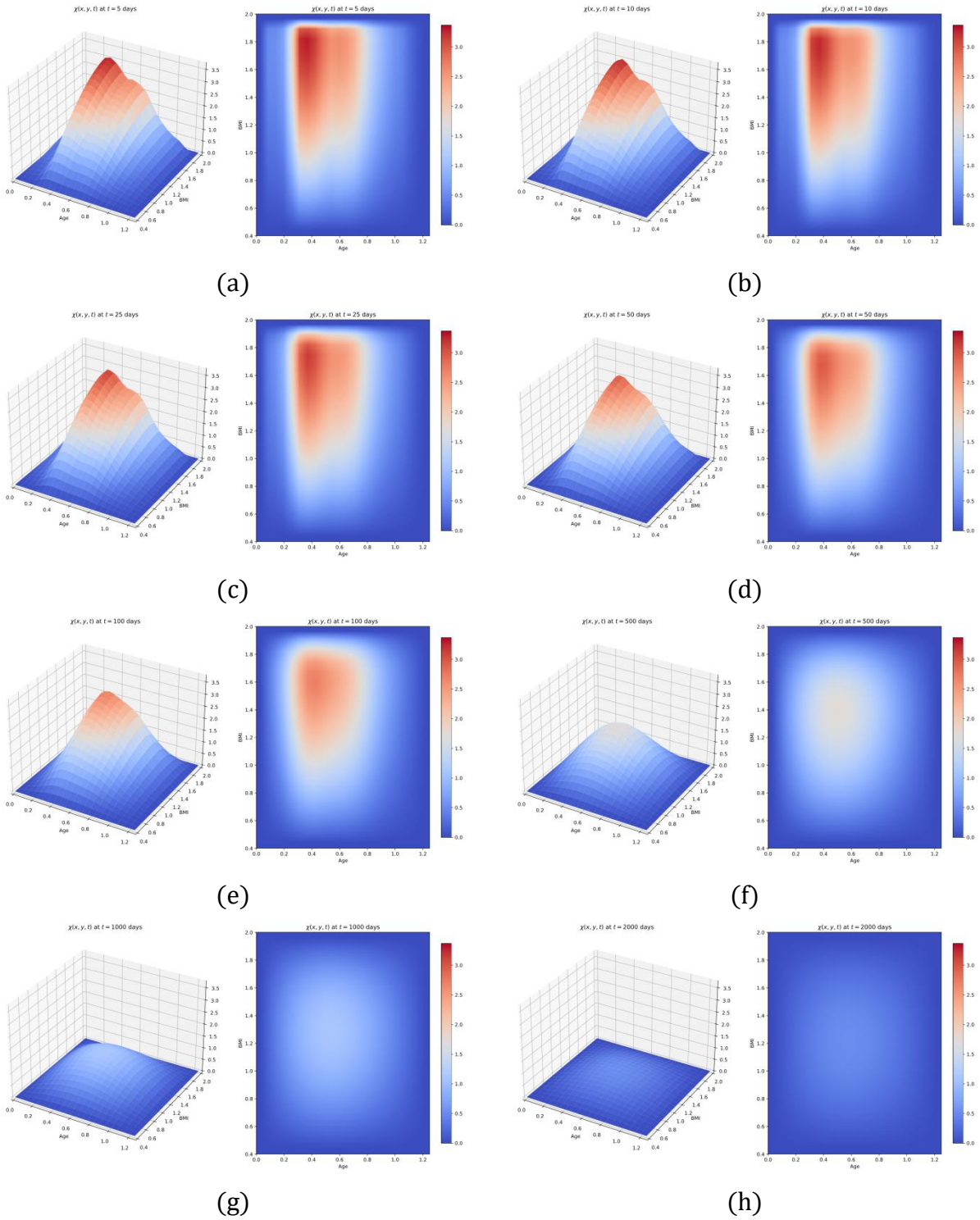

Figure 4: Prospective dynamic evolution of COVID-19 infected fraction $\chi_i = \chi_i(x,y,t)$ as numerically simulated by imposing null Dirichlet condition at all domain boundaries ('healthy perimeter') after: (a) 5 days, (b) 10 days, (c) 25 days, (d) 50 days, (e) 100 days, (f) 500 days, (g) 1000 days, (h) 2000 days

4.6. Paradigm shift in epidemiological dataset

By combining transport phenomena ideas and (dimensionless) generalized coordinates to categorize people, the proposed epidemic transport model is a pioneering framework (to the best of authors' knowledge). Epidemiological dataset for validation purposes should not only describe infectious disease dynamics (not limited to mortality rates) but also characterize its spreading as separated in terms of people's age, comorbidities, activity level, etc.

For numerical simulations in previous section, data from (Florida Department of Health, 2019) could provide an initial scenario as infected people were divided into age groups to some extent. While those data cannot be strictly used for validation, prospective COVID-19 spreading dynamics was successfully simulated with no loss of generality by relying on an innovative (and hopefully promising) epidemiological model framework.

By providing preliminary applications of concepts here discussed, aforesaid numerically simulated scenarios can be stepping-stones for future studies using more complete versions of the epidemic transport equation as epidemiological data become categorized. Unfortunately, COVID-19 pandemic still prevails and categorized dataset might indeed become available for future validation.

4.6. Future developments

While the present work introduces a preliminary epidemic transport model, prospective developments can definitely be envisaged. The following list of theoretical points to ponder is evidently far from exhaustive.

- *Extension to multidimensional models*: many dimensionless generalized coordinates could in principle be invoked in multidimensional (n-D) modeling to include other comorbidities or even cardinal directions themselves.
- *Inhomogeneous hosting media*: diffusivity can be extended to non-uniform media (i.e. $D_{xx} \neq D_{yy}$). It can equally depend on generalized coordinates (i.e. spreading among youth ≠ spreading among elderly) and/or time (i.e. spreading reduces as population becomes more conscious about social distancing).
- *Mixed boundary conditions*: different conditions can in principle be imposed at domain boundaries as exploratory studies of dissimilar infection scenarios.
- *Unbalanced source-sink terms*: different outcomes are expected whenever contamination-reinfection and recovery-death rates are not in equilibrium.
- *Hosting media rheology*: by reminding that viscosity refers to friction forces in fluid flow, what should be its role in an epidemic transport model? From rheological viewpoint, could Newtonian or non-Newtonian fluid flows be associated to different streamwise infection mechanisms? For instance, could latency period be somehow modeled as Bingham plastic?

- *Porous hosting media*: as porosity is a transport property measuring void fraction (clear spaces), could it be a measure of crowding trends? Furthermore, what should be the role of permeability in view of preferential pathways and connectivity among categorized people?
- *Multicomponent-multiphase hosting media*: could this idea be adapted in order to model asymptomatic people as mixed up with symptomatic and not-infected ones?
- *Rarefied hosting media*: if continuum hypothesis no longer holds, could Knudsen diffusion be invoked or adapted to disease spreading? To what extent could this limiting model refer to classic compartmental epidemic models (e.g., SIR, SIS, SEIR, SEIS, SEIRS)?

5. Conclusion

Mathematical epidemiology is a multifaceted science branch whose comprehensiveness is prone to rely on synergy among not only exact and life sciences (as its name suggests) but also social sciences (e.g. human ontology). This is particularly true in view of the epidemic transport model proposed in the present work, in which diffusive (i.e. random infection) and convective (i.e. streamwise infection) contributions are both modeled in terms of categorized people, besides the usual time-dependence.

Momentum, mass and heat transfer have underlying (and ubiquitous) ideas that can be shared and exploited towards mathematical epidemiology. This is because infected people can be equally analyzed and modeled with the help of basic conservation principles together with constitutive equations. By profiting from well-established governing equations typical to transport phenomena, challenges as well as opportunities become broadly open to research on infectious disease spreading. The preliminary epidemic transport model put forward in this work can be a stepping-stone.

Declarations of interest: none.

Acknowledgement

This study is financed in part by the Coordenação de Aperfeiçoamento de Pessoal de Nível Superior - Brasil (CAPES) - Finance code 001.

References

Acuña-Zegarra, M. A., Santana-Cibrian, M., & Velasco-Hernandez, J. X. (2020). Modeling behavioral change and COVID-19 containment in Mexico: A trade-off between lockdown and compliance. Mathematical Biosciences, 325, 108370. https://doi.org/10.1016/j.mbs.2020.108370

Aniţa, L. I., Aniţa, S., 2005. Note on the stabilization of a reaction-diffusion model in epidemiology. Nonlinear Analysis: Real World Applications, 6(3), 537-544. https://doi.org/10.1016/j.nonrwa.2004.11.003

Bailey, N. T. J. (1975). The mathematical theory of infectious diseases and its applications, 2nd ed. Charles Griffin, Glasgow.

Baqui, P., Bica, I., Marra, V., Ercole, A., & van der Schaar, M. (2020). Ethnic and regional variations in hospital mortality from COVID-19 in Brazil: a cross-sectional observational study. The Lancet Global Health, 8, e1018-e1026. https://doi.org/10.1016/S2214-109X(20)30285-0

Barton, P. I. (1992). The Modelling and Simulation of Combined Discrete/Continuous Processes. Ph.D. thesis. University of London, UK.

Belik, V., Geisel, T., & Brockmann, D. (2011). Recurrent host mobility in spatial epidemics: beyond reaction-diffusion. The European Physical Journal B, 84, 579-587. https://doi.org/10.1140/epjb/e2011-20485-2

Bennett, C. O., & Myers, J. E. (1974). Momentum, Heat and Mass Transfer, 2nd ed. McGraw-Hill, New York.

Bevand, M. (2020). Forecasting deaths and analyzing age trends of COVID-19 cases in Florida. Github Page. https://github.com/mbevand/florida-covid19-line-list-data (accessed 12 January 2021).

Binda, B., Picchi, G., Carucci, A. C., Sinatti, G., Di Norcia, M., Grimaldi, A., Lancione, L., Natili, A., Chiappori, D., Montali, F., Lupi, D., Martinez, V., Panarese, A., D'anselmi, F., & Pisani, F. (2020). Follow-up and management of kidney transplant recipients during the COVID-19 lockdown: the experience of an Italian transplant center, including two cases of COVID-19 pneumonia. Transplantation Proceedings, 52(9), 2614-2619. https://doi.org/10.1016/j.transproceed.2020.06.026

Bird, R. B., Lightfoot, E. N., & Stewart, W. E. (2007). Transport Phenomena, revised 2nd ed. John Wiley & Sons, Hoboken.

Blyuss, K. B., & Kyrychko, Y. N. (2021). Effects of latency and age structure on the dynamics and containment of COVID-19. Journal of Theoretical Biology, 513, 110587. https://doi.org/10.1016/j.jtbi.2021.110587

Brauer, F., & Castillo-Chávez, C. (2012). Mathematical Models in Population Biology and Epidemiology, 2nd ed. Springer-Verlag, New York.

Britton, T., Ball, F., & Trapman, P. (2020). A mathematical model reveals the influence of population heterogeneity on herd immunity to SARS-CoV-2. Science, 369(6505), 846-849. DOI: 10.1126/science.abc6810

Chekroun, A., & Kuniya, T. (2020). Global threshold dynamics of an infection age-structured SIR epidemic model with diffusion under the Dirichlet boundary condition. Journal of Differential Equations, 269(8), 117-148. https://doi.org/10.1016/j.jde.2020.04.046

Crank, J. (1975). The Mathematics of Diffusion, 2nd ed. Oxford University Press, Oxford.

Cussler, E. L. (2009). Diffusion – Mass Transfer in Fluid Systems, 3rd ed. Cambridge University Press, Cambridge.

Dai, F., & Liu, B. (2020). Optimal control problem for a general reaction-diffusion eco-epidemiological model with disease in prey. Applied Mathematical Modelling, 88, 1-20. https://doi.org/10.1016/j.apm.2020.06.040

Danckwerts, P. V. (1953). Continuous flow systems. Distribution of residence times. Chemical Engineering Science, 2, 1-13. https://doi.org/10.1016/0009-2509(53)80001-1

David, S. A., & Rabi, J. A. (2020). Can fractional calculus be applied to relativity? Axiomathes, 30, 165-176. https://doi.org/10.1007/s10516-019-09448-9

de Souza-Santos, M. L. (2010). Solid Fuels Combustion and Gasification: Modeling, Simulation, and Equipment Operations, 2nd ed. CRC Press, Boca Raton.

Docherty, A. B., Mulholland, R. H., Lone, N. I., Cheyne, C. P., de Angelis, D., Diaz-Ordaz, K., Donegan, C., Drake, T. M., Dunning, J., Funk, S., García-Fiñana, M., Girvan, M., Hardwick, H. E., Harrison, J., Ho, A., Hughes, D. M., Keogh, R. H., Kirwan, P. D., Leeming, G., Van-Tam, J. S. N., Pius, R., Russell, C. D., Spencer, R. G., Tom, B. D. M., Turtle, L., Openshaw, P. J. M., Baillie, J. K., Harrison, E. M., Semple, M. G., & ISARIC4C Investigators (2021). Changes in in-hospital mortality in the first wave of COVID-19: a multicentre prospective observational cohort study using the WHO Clinical Characterisation Protocol UK. The Lancet Respiratory Medicine, online. https://doi.org/10.1016/S2213-2600(21)00175-2

Donadello, C., Nguyen, T. N. T., & Razafison, U. (2021). On the mathematical modeling of vole populations spatial dynamics via transport equations on a graph. Applied Mathematics and Computation, 396, 125885. https://doi.org/10.1016/j.amc.2020.125885

Ducrot, A., & Magal, P. (2009). Travelling wave solutions for an infection-age structured model with diffusion. Proceedings of the Royal Society of Edinburgh. Section A: Mathematics, 139(3), 459-482. https://doi.org/10.1017/S0308210507000455

Florida Department of Health, Bureau of Community Health Assessment, Division of Public Health Statistics and Performance Management (2019). Life Expectancy Report. http://www.flhealthcharts.com/ChartsReports/rdPage.aspx?rdReport=ChartsProfiles.LifeExpectancyProfile (accessed 01 January 2021).

Florida Department of Health, Division of Disease Control and Health Protection (2020). Case line data for COVID-19 confirmed cases in the state of Florida, updated daily. https://www.arcgis.com/home/item.html?id=4cc62b3a510949c7a8167f6baa3e069d (accessed 12 January 2021).

Gadzik, J. (2006). "How much should I weigh?" -- Quetelet's equation, upper weight limits, and BMI prime. Connecticut Medicine, 70(2), 81-88. PMID: 16768059

Hamid, S., Mir, M. Y., & Rohela, G. K. (2020). Novel coronavirus disease (COVID-19): a pandemic (epidemiology, pathogenesis and potential therapeutics). New Microbes and New Infections, 35, 100679. https://doi.org/10.1016/j.nmni.2020.100679

Hethcote, H. W. (1989). Three Basic Epidemiological Models. In: Levin, S. A., Hallam, T. G., & Gross, L. J. (Eds.), Applied Mathematical Ecology - Biomathematics, v. 18. Springer, Berlin-Heidelberg, pp. 119-144.

Hines, A. L., & Maddox, R. N. (1985). Mass Transfer: Fundamentals and Applications. Prentice-Hall, Upper Saddle River.

Kaviany, M. (1995). Principles of Heat Transfer in Porous Media, 2nd ed. Springer-Verlag, New York.

Kays, W. M., Crawford, M. E., & Weigand, B. (2005). Convective Heat and Mass Transfer. McGraw-Hill, New York.

Kermack, W. O., & McKendrick, A. G. (1927). A contribution to the mathematical theory of epidemics. Proceedings of the Royal Society A: Mathematical, Physical and Engineering Sciences, 115(772), 700-721. https://doi.org/10.1098/rspa.1927.0118

Kraemer, M. U. G., Yang, C. H., Gutierrez, B., Wu, C. H., Klein, B., Pigott, D. M., Open COVID-19 Data Working Group, Plessis, L., Faria, N. R., Li, R., Hanage, W. P., Brownstein, J. S., Layan, M.,

Vespignani, A., Tian, H., Dye, C., Pybus, O. G., & Scarpino, S. V. (2020). The effect of human mobility and control measures on the COVID-19 epidemic in China. Science, 368(6490), 493-497. DOI: 10.1126/science.abb4218.

Kreyszig, E. (2011). Advanced Engineering Mathematics, 10th ed. John Wiley & Sons, Hoboken.

Leal, L. G. (2007). Advanced Transport Phenomena: Fluid Mechanics and Convective Transport Processes, v. 7. Cambridge University Press, Cambridge.

Levesque, J., Maybury, D. W., & David Shaw, R. H. A. (2021). A model of COVID-19 propagation based on a gamma subordinated negative binomial branching process. Journal of Theoretical Biology, 512, 110536. https://doi.org/10.1016/j.jtbi.2020.110536

May, S. (2017). Spacetime discontinuous Galerkin methods for solving convection-diffusion systems. ESAIM: Mathematical Modelling and Numerical Analysis, 51(5), 1755-1781. https://doi.org/10.1051/m2an/2017001

Medlock, J. P. (2004). Integro-differential-equation models in ecology and epidemiology. Ph.D. thesis. University of Washington, USA.

Monod, M., Blenkinsop, A., Xi, X., Hebert, D., Bershan, S., Tietze, S., Baguelin, M., Bradley, V. C., Chen, Y., Coupland, H., Filippi, S., Ish-Horowicz, J., McManus, M., Mellan, T., Gandy, A., Hutchinson, M., Unwin, H. J. T., van Elsland, S. L., Vollmer, M. A. C., Weber, S., Zhu, H., Bezancon, A., Ferguson, N. M., Mishra, S., Flaxman, S., Bhatt, S., Ratmann, O., & Imperial College COVID-19 Response Team (2021). Age groups that sustain resurging COVID-19 epidemics in the United States. Science, 371(6536), eabe8372. DOI: 10.1126/science.abe8372

Morse, P. M., & Feshbach, H. (1953). Methods of Theoretical Physics, Part I. McGraw-Hill, New York.

Nield, D. A., & Bejan, A. (2017). Convection in Porous Media, 5th ed. Springer, New York.

Overton, C. E., Stage, H. B., Ahmad, S., Curran-Sebastian, J., Dark, P., Das, R., Fearon, E., Felton, T., Fyles, M., Gent, N., Hall, I., House, T., Lewkowicz, H., Pang, X., Pellis, L., Sawko, R., Ustianowski, A., Vekaria, B., & Webb, L. (2020). Using statistics and mathematical modelling to understand infectious disease outbreaks: COVID-19 as an example. Infectious Disease Modelling, 5, 409e441. https://doi.org/10.1016/j.idm.2020.06.008

Ørstavik, S., Carretero-González, R., & Stark, J. (2000). Estimation of intensive quantities in spatio-temporal systems from time-series. Physica D: Nonlinear Phenomena, 147(3-4), 204-220. https://doi.org/10.1016/S0167-2789(00)00166-4

Peube, J. L. (2009). Fundamentals of Fluid Mechanics and Transport Phenomena. ISTE, London – John Wiley & Sons, Hoboken.

Richardson, S., Hirsch, J. S., Narasimhan, M., Crawford, J. M., McGinn, T., Davidson, K. W., & Northwell COVID-19 Research Consortium (2020). Presenting characteristics, comorbidities, and outcomes among 5700 patients hospitalized with COVID-19 in the New York city area. Journal of the American Medical Association, 323(20), 2052-2059. DOI: 10.1001/jama.2020.6775

Riley, K. F., Hobson, M. P., & Bence, S. J. (2006). Mathematical Methods for Physics and Engineering, 3rd ed. Cambridge University Press, Cambridge.

Rodi, W. (2017). Turbulence modeling and simulation in hydraulics: A historical review. Journal of Hydraulic Engineering, 143(5), 03117001. https://doi.org/10.1061/(ASCE)HY.1943-7900.0001288

Rosenberg, N. A. (2021). Editorial – Population models, mathematical epidemiology, and the COVID-19 pandemic. Theoretical Population Biology, 137, 1. https://doi.org/10.1016/j.tpb.2021.01.001

Sabel, C. E., Pringle, D., & Schærström, A. (2009). Infectious Disease Diffusion. In: Brown, T., McLafferty, S., Moon, G. (Eds.), A companion to health and medical geography. Blackwell Publishing Ltd., Oxford, pp. 111-132.

Saguy, I. S. (2016). Challenges and opportunities in food engineering: Modeling, virtualization, open innovation and social responsibility. Journal of Food Engineering, 176, 2-8. http://dx.doi.org/10.1016/j.jfoodeng.2015.07.012

Shaw, C. L., & Kennedy, D. A. (2021). What the reproductive number can and cannot tell us about COVID-19 dynamics. Theoretical Population Biology, 137, 2-9. https://doi.org/10.1016/j.tpb.2020.12.003

Shen, M., Peng, Z., Xiao, Y., & Zhang, L. (2020). Modeling the epidemic trend of the 2019 novel coronavirus outbreak in China. The Innovation, 1, 100048. https://doi.org/10.1016/j.xinn.2020.100048

Sissom, L. E., Pitts, D. R. (1972). Elements of Transport Phenomena. McGraw-Hill, New York.

Skelland, A. H. P. (1974). Diffusional Mass Transfer. John Wiley & Sons, New York.

Slattery, J. C., Sagis, L., & Oh, E. S. (2007). Interfacial Transport Phenomena. Springer Science & Business Media, Boston.

White, F. M. (2006). Viscous Fluid Flow, 3rd ed. McGraw-Hill, New York.

WHO – World Health Organization (2020a). Coronavirus disease (COVID-19) pandemic. https://www.euro.who.int/en/health-topics/health-emergencies/coronavirus-covid-19/novel-coronavirus-2019-ncov (accessed 14 July 2020).

WHO – World Health Organization (2020b). Coronavirus disease 2019 (COVID-19) situation report – 92. https://www.who.int/emergencies/diseases/novel-coronavirus-2019/situation-reports (accessed 14 July 2020).

WHO – World Health Organization (2020c). Report of the WHO-China Joint Mission on Coronavirus Disease 2019 (COVID-19). https://www.who.int/docs/default-source/coronaviruse/who-china-joint-mission-on-covid-19-final-report.pdf (accessed 14 July 2020).

Wiersinga, W. J., Rhodes, A., Cheng, A. C., Peacock, S. J., & Prescott, H. C. (2020). Pathophysiology, transmission, diagnosis, and treatment of coronavirus disease 2019 (COVID-19): a review. Journal of the American Medical Association, 324(8), 782-793. DOI: 10.1001/jama.2020.12839

Zhu, N., Zhang, D., Wang, W., Li, X., Yang, B., Song, J., Zhao, X., Huang, B., Shi, W., Lu, R., Niu, P., Zhan, F., Ma, X., Wang, D., Xu, W., Wu, G., Gao, G. F., & Tan, W. (2020). A novel coronavirus from patients with pneumonia in China, 2019. The New England Journal of Medicine, 382(8), 727-733. DOI: 10.1056/NEJMoa2001017